UNIVERSITY OF BIRMINGHAM
University of Birmingham Research at Birmingham

Generation of stem cell-based bioartificial anterior cruciate ligament (ACL) grafts for effective ACL rupture repair

Kouroupis, Dimitrios; Kyrkou, Athena; Triantafyllidi, Eleni; Katsimpoulas, Michalis; Chapelakis, George; Goussia, Anna; Georgoulis, Anastasios; Murphy, Carol; Fotsis, Theodore

DOI:
10.1016/j.scr.2016.04.016

License:
Creative Commons: Attribution-NonCommercial-NoDerivs (CC BY-NC-ND)

Document Version
Publisher's PDF, also known as Version of record

Citation for published version (Harvard):
Kouroupis, D, Kyrkou, A, Triantafyllidi, E, Katsimpoulas, M, Chapelakis, G, Goussia, A, Georgoulis, A, Murphy, C & Fotsis, T 2016, 'Generation of stem cell-based bioartificial anterior cruciate ligament (ACL) grafts for effective ACL rupture repair', *Stem Cell Research*. https://doi.org/10.1016/j.scr.2016.04.016

Link to publication on Research at Birmingham portal

General rights
Unless a licence is specified above, all rights (including copyright and moral rights) in this document are retained by the authors and/or the copyright holders. The express permission of the copyright holder must be obtained for any use of this material other than for purposes permitted by law.

• Users may freely distribute the URL that is used to identify this publication.
• Users may download and/or print one copy of the publication from the University of Birmingham research portal for the purpose of private study or non-commercial research.
• User may use extracts from the document in line with the concept of 'fair dealing' under the Copyright, Designs and Patents Act 1988 (?)
• Users may not further distribute the material nor use it for the purposes of commercial gain.

Where a licence is displayed above, please note the terms and conditions of the licence govern your use of this document.

When citing, please reference the published version.

Take down policy
While the University of Birmingham exercises care and attention in making items available there are rare occasions when an item has been uploaded in error or has been deemed to be commercially or otherwise sensitive.

If you believe that this is the case for this document, please contact UBIRA@lists.bham.ac.uk providing details and we will remove access to the work immediately and investigate.

Download date: 01. Mar. 2020

Stem Cell Research xxx (2016) xxx–xxx

Contents lists available at ScienceDirect

Stem Cell Research

journal homepage: www.elsevier.com/locate/scr

Generation of stem cell-based bioartificial anterior cruciate ligament (ACL) grafts for effective ACL rupture repair

Dimitrios Kouroupis [a,1], Athena Kyrkou [a,1], Eleni Triantafyllidi [b], Michalis Katsimpoulas [c,d], George Chalepakis [e], Anna Goussia [b], Anastasios Georgoulis [f], Carol Murphy [a,g], Theodore Fotsis [a,g,h,*]

[a] Department of Biomedical Research, Institute of Molecular Biology & Biotechnology, Foundation of Research and Technology-Hellas, University Campus, 45110 Ioannina, Greece
[b] Department of Pathology, University of Ioannina, 45110 Ioannina, Greece
[c] Centre of Clinical, Experimental Surgery and Translational Research, Experimental Surgery Unit, Biomedical Research Foundation of the Academy of Athens, 11527 Athens, Greece
[d] Attikon animal hospital, 19002, Paiania, Athens, Greece
[e] Department of Biology, Electron microscopy laboratory, University of Crete, 70013 Heraklion, Greece
[f] Orthopaedic Sports Medicine Center-Department of Orthopaedic Surgery, University of Ioannina, 45110 Ioannina, Greece
[g] School of Biosciences, College of Life and Environmental Sciences, University of Birmingham, Edgbaston, Birmingham, B15 2TT, UK
[h] Laboratory of Biological Chemistry, Medical School, University of Ioannina, 45110 Ioannina, Greece

ARTICLE INFO

Article history:
Received 22 December 2015
Received in revised form 11 April 2016
Accepted 20 April 2016
Available online xxxx

Keywords:
Anterior cruciate ligament reconstruction
Human adipose tissue multipotential stromal cells
Human induced pluripotent stem cells
Biomaterials
Tissue engineering
Bioartificial ACL graft

ABSTRACT

In the present study, we combined stem cell technology with a non-absorbable biomaterial for the reconstruction of the ruptured ACL. Towards this purpose, multipotential stromal cells derived either from subcutaneous human adipose tissue (hAT-MSCs) or from induced pluripotent stem cells (iPSCs) generated from human foreskin fibroblasts (hiPSC-MSCs) were cultured on the biomaterial for 21 days *in vitro* to generate a 3D bioartifical ACL graft. Stem cell differentiation towards bone and ligament at the ends and central part of the biomaterial was selectively induced using either BMP-2/FGF-2 or TGF-β/FGF-2 combinations, respectively. The bioartificial ACL graft was subsequently implanted in a swine ACL rupture model in place of the surgically removed normal ACL. Four months post-implantation, the tissue engineered ACL graft generated an ACL-like tissue exhibiting morphological and biochemical characteristics resembling those of normal ACL.

© 2016 The Authors. Published by Elsevier B.V. This is an open access article under the CC BY-NC-ND license (http://creativecommons.org/licenses/by-nc-nd/4.0/).

1. Introduction

Regenerative medicine (RM) is an interdisciplinary field of research and clinical applications focus on the repair, replacement, or regeneration of cells, tissues and organs to restore impaired function. RM employs technological breakthroughs such as those used in tissue engineering (TE) (*i.e.* biodegradable, biomimetic biopolymers, nanotechnology, biosensors etc) in combination with the powerful differentiation capacity of stem cells. Indeed, adipose tissue (AT) is a rich source of multipotential stromal cells (MSCs) that can be successfully differentiated towards mesoderm-related lineages such as osteoblasts, adipocytes, chondroblasts and fibroblasts representing a good overall option for autologous regenerative applications. Adult tissues, however, contain only committed stem cells that are multi- or even oligopotent. The use of human embryonic stem cells (hESCs) for medical applications is prohibited for legal/ethical (commercialization of life) and medical (immune rejection of heterologous tissue) reasons. Thus, generation of induced pluripotent stem cells (iPSCs) by reprogramming of terminally differentiated cells (Takahashi and Yamanaka, 2006) offers the possibility for autologous regeneration of any tissue using pluripotent stem cells.

Anterior cruciate ligament (ACL) is critical for the stability of the knee and ACL rupture results in meniscal and cartilage damage leading to early osteoarthritis. Current repair methods suffer from the low healing capacity of the ACL, and from the postoperative consequences of ACL reconstruction approaches, such as osteoarthritis (OA) (Leong et al., 2013), originate from modified joint mechanics as a result of lack of fidelity in the anatomic insertion and alignment of the ligament, and loss of tissue with neurosensory function (Kiapour and Murray, 2014). The combined potential of RM and TE can be used both in repair and reconstruction ACL therapies. Both had been proven to be a difficult task, but generating a bioartificial ACL poses a particular challenge due

DOI of original article: http://dx.doi.org/10.1016/j.scr.2016.05.006.
* Corresponding author at: Department of Biomedical Research, Institute of Molecular Biology & Biotechnology, Foundation of Research and Technology-Hellas, University Campus, 45110 Ioannina, Epirus, Greece.
E-mail address: thfotsis@uoi.gr (T. Fotsis).
[1] Co-first author.

http://dx.doi.org/10.1016/j.scr.2016.04.016
1873-5061/© 2016 The Authors. Published by Elsevier B.V. This is an open access article under the CC BY-NC-ND license (http://creativecommons.org/licenses/by-nc-nd/4.0/).

Please cite this article as: Kouroupis, D., et al., Generation of stem cell-based bioartificial anterior cruciate ligament (ACL) grafts for effective ACL rupture repair, Stem Cell Res. (2016), http://dx.doi.org/10.1016/j.scr.2016.04.016

ARTICLE IN PRESS

to its structure and anatomy. Indeed, the tissue engineered construct has to be induced to differentiate towards a fibrous middle part representing the ACL ligament and two osseous components, one at each end of the construct, forming the bone attachment points. To the best of our knowledge, such an approach, closely simulating the structure of the human ACL has not been reported in the literature. Thus, in the present study, we have evaluated the possibility of developing a tissue engineered construct for the regeneration of ACL based on the above approach establishing the appropriate conditions and comparing the suitability of hAT-MSCs and hiPSC-MSCs for this purpose.

2. Materials & methods

The derivation and culturing conditions of hAT-MSCs are thoroughly described in Supplementary Materials and methods section, while details regarding hiPS lines generation and validation are described elsewhere (Kyrkou et al., in press).

2.1. Phenotypic characterisation of hiPS-MSCs and hAT-MSCs

Phenotypic characterisation of cultured MSCs was performed at passage 3 to evaluate the expression of markers specific for MSC, haematopoietic, and endothelial lineages (PE-conjugated antibodies and isotypes in Supplementary Table 4). Flow cytometry was performed using CyFlow (Partec, Münster, Germany). Briefly, a total of 2×10^5 cultured cells were stained with PE-conjugated antibodies, and dead cells were excluded using 2 μg/ml 7-Amino-actinomycin D (7-AAD) viability staining solution (Invitrogen).

2.2. Multipotency of hiPS-MSCs and hAT-MSCs

Cultured MSCs were expanded *in vitro* under standard conditions to passage 3 (p3) and then subjected to differentiation induction protocols. Osteogenic differentiation was performed using standard osteoinduction conditions and semi-quantitative assessment of osteoblast differentiation was performed using the alkaline phosphatase (ALP) activity assay. Visual assessment of mineralisation was performed using Alizarin Red S (Sigma) (Jones et al., 2002). Chondrogenic differentiation was performed using standard protocols in pellet cultures and semi-quantitative assessment of chondrogenesis was performed using Toluidine blue stain (Sigma) (Jones et al., 2002). Adipogenic differentiation was performed using standard adipoinduction conditions and evaluated using 0.5% Oil Red (Sigma) as previously described (Jones et al., 2002). Quantitative real-time PCR (qPCR) to investigate transcript expression of hAT-MSCs and hiPS-MSCs is described in Supplementary Materials and methods section.

2.3. Human AT-MSC seeding on biomaterial and differentiation towards ligament and osteogenic cells

Matrigel was thawed for 24 h at 4 °C. Passage 3 hAT-MSCs were trypsinised (as described above), centrifuged and embedded in thawed Matrigel matrix at a ratio of 2×10^6 cells per 100 μl. The hAT-MSCs/Matrigel mix was placed on the Leeds-Keio biomaterial (static seeding). On day 7 post-seeding the construct was rinsed with PBS, fixed with 10% formaldehyde for 10 min and stained with YOYO-1 (1:10,000, Invitrogen) for 20 min. The morphology and attachment of the cells on the biomaterial was visualised by Leica TCS SP5 confocal microscope (10× dry objective).

Three dimensional differentiation of hAT-MSCs on Leeds-Keio was performed in a way to closely mimic normal human ACL's structure compartmentalisation *in vivo*. Two separate induction strategies were employed. Ligament-induction was assessed by mixing 1×10^6 cells with 5 ng/ml TGF-β and 3 ng/ml FGF-2 (both from PeproTech, Rocky Hill, USA) and embedding them in 50 μl Matrigel (LMC). Osteogenic-induction was assessed by mixing 1×10^6 cells with 100 ng/ml BMP-2 (PeproTech) and 3 ng/ml FGF-2 and embedding them in 50 μl Matrigel matrix (OMC). The LMC was directly applied to the central part of the biomaterial whereas OMC was directly applied to the lateral ends of the biomaterial, and left to solidify on the biomaterial for 20 min at 37 °C in a 100 mm dish. Medium was refreshed every 72 h with ADSC (Lonza) and the differentiation assay was terminated at day 21. The whole transcriptome molecular profiling of hAT-MSC implants is described in Supplementary Materials and methods section.

2.4. Human iPS-MSC seeding on biomaterial and differentiation towards ligament and osteogenic cells

Human iPS were precommitted towards mesodermal fate by gradually replacing mTeSR with ADSC expansion medium. Briefly, after manual passaging hiPS' clumps were seeded on standard culture matrigel coated dishes. The first 2 days cells were fed with mTeSR, the following 2 days mTeSR was diluted 4:1 with ADSC medium. Day 5–6 the dilution was 1:1 and the last 2 days 1:4. Committed cells (hiPS-MSCs) were trypsinised, neutralised, centrifuged and resuspended in 100 μl of ADSC medium. Resuspended cells were split into two equal fractions each one used to form the ligament-induction and osteogenic-induction strategies, respectively. Three dimensional differentiation of committed cells on Leeds-Keio was performed as described above. The whole transcriptome molecular profiling of hiPS-MSC implants is described in Supplementary Materials and methods section.

2.5. Implant placement in a swine ACL injury model

Six Landrace × Large White swine (3 months old, 25–30 kg) were divided into experimental groups: three animals were treated with hiPS-MSC/biomaterial implant, two animals with hAT-MSC/biomaterial implant, and one animal with biomaterial alone. Both ends of shaft were sutured with double leader line 80 lb. (Veterinary Instrumentation, Sheffield, UK). The lateral parapatellar arthrotomy was used to expose the right knee joint and specially the ACL, without harming the fat pad or other tissues of the knee joint. After the excision of the ACL, the femoral and tibial bone tunnels were created with a 5.0 mm diameter drill bit. The shaft was passed through the bone tunnel and joint cavity and both ends were fixed by crimp clamp at the lateral side of the joint flexed at 30° with the implant in slight tension. Four months post-surgery, the animals were euthanised with a bolus dose of pentobarbital sodium euthanasia solution (Dolethal, Vetoquinol) at a dose of 2 ml/kg and the whole knee was removed for morphological and immunohistochemical evaluation of ACL reconstruction. The anatomical preparation, sequencing and histological analysis of ACL tissues is described in Supplementary Materials and methods section.

3. Results

3.1. Mesodermal commitment of hiPSCs

Human iPSCs were committed to the mesodermal lineage by replacing mTESR with ADSC medium and gradually increasing the FCS concentration to 10% (Fig. 1A). This commitment protocol resulted in the generation of two MSC-like populations, early and late MSC-like cells (hiPS-MSCs), 10 and 20 days post-induction, respectively. hiPSC cell colonies gradually became round CFU-F colonies containing characteristic MSC-like spindle shaped cells (Fig. 1B). The CFU-F yield was 239, 291, 256 colonies per 10^4 cells seeded at passage 3 for hiPS-MSC lines 1, 2 and 3, respectively. Single cells representing the stem cell population were gated (R1), excluding cell doublets and cell debris from our analysis, and constituted the first step of the gating strategy leading to distinct cell populations (A1, A2) generated by staining with PE-conjugated specific markers against cell surface epitopes (Fig. 1C). Surface phenotyping of hiPSC-MSCs was carried out using an abundance of surface markers used to characterise passage 3 hAT-MSC cultures (see later

Please cite this article as: Kouroupis, D., et al., Generation of stem cell-based bioartificial anterior cruciate ligament (ACL) grafts for effective ACL rupture repair, Stem Cell Res. (2016), http://dx.doi.org/10.1016/j.scr.2016.04.016

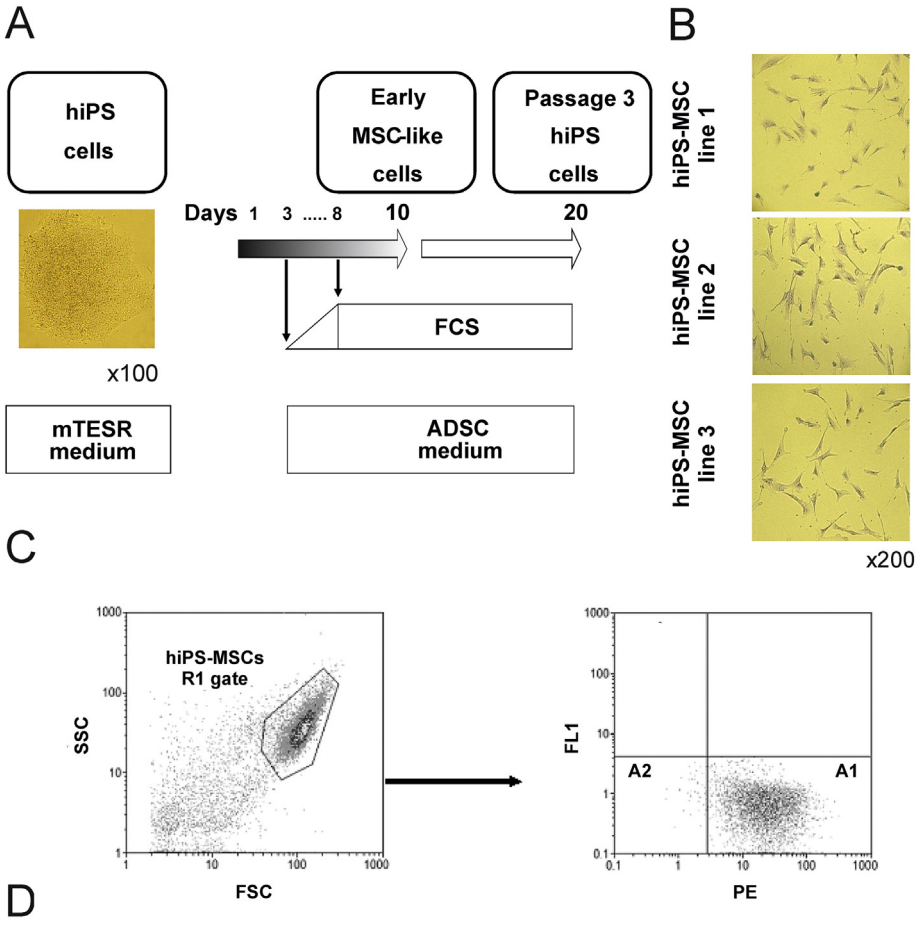

	Pluripotent hiPS			Early MSC-like cells			hiPS-MSCs		
	line 1	line 2	line 3	line 1	line 2	line 3	line 1	line 2	line 3
CD14	0	0	0	0	0	0	0	0	0
CD15	0.18	0.12	0.52	7.75	9.24	10.69	0.81	0.36	0.13
CD29	97.54	97.74	98	99.45	99.52	99.51	99.92	99.63	99.63
CD31	0	0	0	0	0	0	0.38	0.44	0.29
CD34	0	0	0	0	0	0	0.81	0.09	0.09
CD44	15.24	20.75	26.43	87.55	91.81	97.74	99.63	99.27	99.08
CD45	0	0	0	0	0	0	0	0	0
CD73	5.72	10.59	5.98	44.14	34.45	43.82	99.73	98.86	99.15
CD90	20.54	22.94	16.24	30.66	17.62	32.21	32.98	27.87	14.33
CD105	0.2	0.44	0.73	24.88	21.16	15.39	50.15	87.1	98.1
CD115	2.34	3.64	2.68	1.26	6.07	5.99	1.19	0.7	1.34
CD140β	31.51	95.94	86.23	2.43	2.27	3.5	36.88	34.2	44.5
CD146	32.95	38.39	67.14	93.02	90.76	94.66	80.73	96.64	97.47
CD201	0.47	1.55	2.43	25.11	24.52	18.76	53.53	42.77	54.86
CD235α	0	0	0	0	0	0	0	0	0
CD324	67.22	75.96	73.42	46.17	68.73	49.2	14.73	6.4	14.8
CD140α	0.4	0.16	0.16	7.09	5.84	3.75	2.79	7.45	0.97
Ve-cadherin	0.36	0.32	0.04	1.46	2.38	1.84	0.32	0.49	1.2

Fig. 1. Mesodermal commitment of hiPS: A) Commitment protocol of hiPS towards mesenchymal cell fate. B) Colony-Forming-Unit (CFU) assay of generated hiPS-MSCs. CFU-F colonies consisting of at least 50 cells were generated 10 days post-hiPS-MSC seeding *in vitro* C) Gating strategy of two-colour flow cytometry analysis. FSC and SSC parameters were used to gate the actual hiPS-MSC population by excluding all debris, cell doublets and dead cells. All surface markers used were conjugated to PE fluorochrome. D) Phenotypic profiling of hiPS cultures pre- and post-mesodermal commitment. Surface marker phenotyping of hiPS from the pluripotent state, to the early MSC-like state and finally, the late MSC-like state (hiPS-MSCs). Commitment process of hiPS results in gradual decrease of pluripotency markers and acquisition of MSC characteristics.

in the text). In the hiPSC-MSCs the expression of haematopoetic (CD14, CD15, CD45, CD235α) and endothelial cell surface markers (CD31) was very low or absent, whereas key MSC (CD29, CD44, CD73, CD105, CD90) and pericytic (CD201, CD140α and CD140β) markers were highly expressed (Fig. 1D).

Chondrogenic induction of hiPSC-MSCs in 3-D pellet cultures resulted in good chondropellet formation and production of highly sulfated glycosaminoglycans in all three clones (Fig. 2A, upper two rows). Osteogenic induction resulted in the differentiation of hiPS-MSCs into osteoblasts in 2-D cultures that was associated with high ALP activity in all

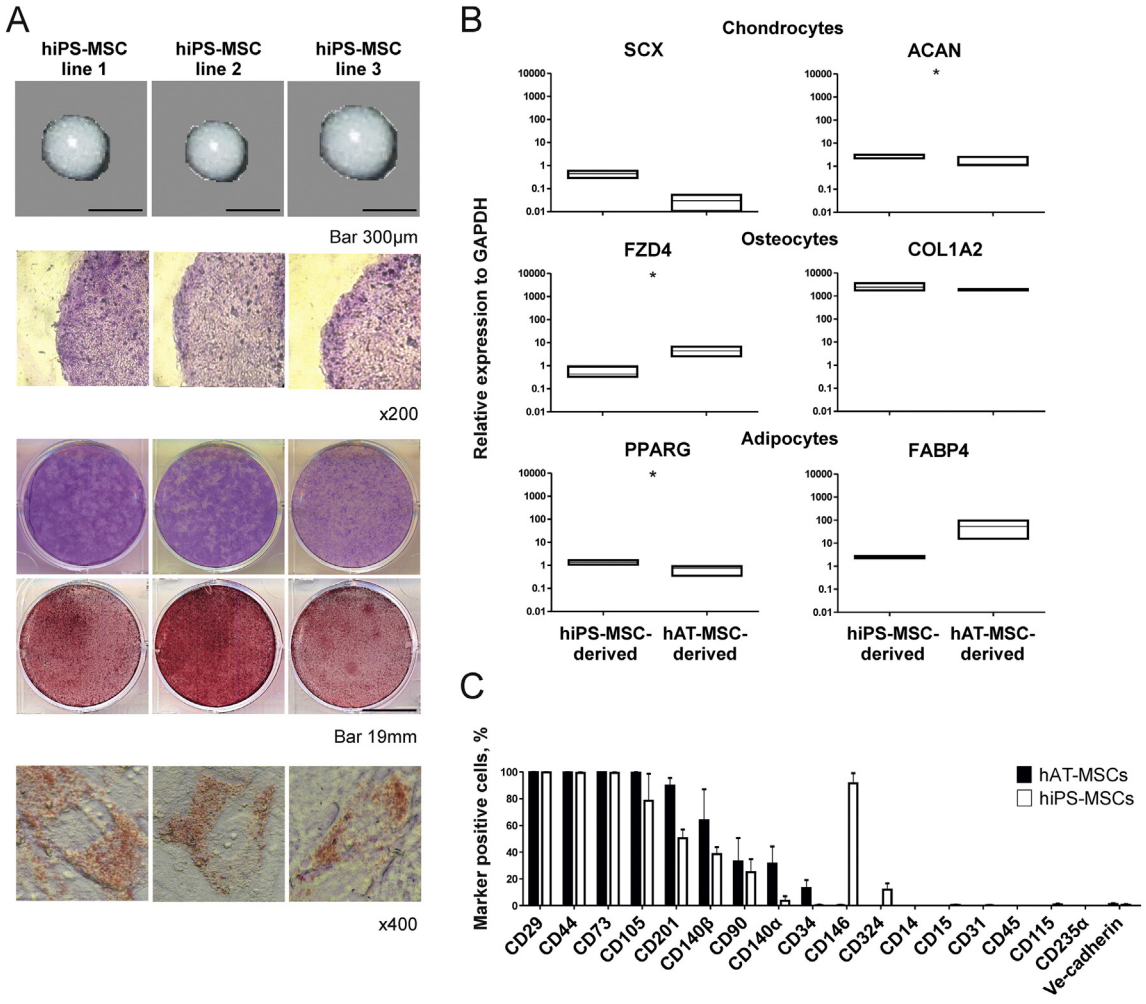

Fig. 2. Multipotentiality of committed hiPS: A) All hiPS-MSC lines showed tripotentiality. Shiny, round chondropellets rich in sGAGs are generated 15 days post-chondroinduction *in vitro* (upper two panels). Osteogenic induction of hiPS-MSCs results in ALP^{+} osteocultures with high levels of mineralisation (middle two panels) on day 21. Multiple, tiny (grade 2) lipid droplets are evident within cell cytoplasm 21 days post-adipoinduction of hiPS-MSC lines. B) qPCR validation of trilineage differentiation (chondrogenesis-, osteogenesis- and adipogenesis-related transcript expression analysis in upper, middle and bottom panels, respectively). All hiPS-MSC lines show upregulation of individual lineage-related transcripts when compared to AT-MSC cultures. C) Generated hiPS-MSCs show similar phenotypic profile to hAT-MSCs. Interestingly, hiPS-MSCs had significantly higher expression levels of CD146 (MSC/endothelial marker) and CD324 (pluripotency marker) compared to hAT-MSCs ($p < 0.05$).

hiPSC-MSC lines and mineral deposition in hiPSC-MSC lines 1 and 2 (Fig. 2A, two middle panels). Adipogenic induction resulted in early adipocyte formation in all hiPS-MSC lines as their lipid accumulation within the cell cytoplasm was limited (Fig. 2A, bottom panel) with adipocytes ranked as grade 2 (English et al., 2007) and differentiation efficiency approx. 20% of the whole culture. Mesodermal commitment of the hiPSC-MSCs to chondrogenic, osteogenic and adipogenic directions was complemented with evaluation of early and late lineage-specific molecules of each mesodermal lineage (Fig. 2B). The progress of mesodermal commitment of hiPS indicated the gradual loss of pluripotency (Supplementary Fig. 2). The expression of CD324 pluripotency marker molecule (Li et al., 2010) was gradually decreased during mesodermal commitment of hiPS as expected, suggesting the mesoderm-restricted profile of the generated hiPS-MSCs. Differentiation of hiPS to hiPS-MSC lines did not induce chromosomal abnormalities as seen by CGH analysis (Supplementary Fig. 1B).

3.2. Isolation, characterisation and further mesodermal differentiation of hAT-MSCs

We have used the stromal-vascular fraction (SVF) of supra-adventitial and perivascular areas (Zimmerlin et al., 2013) to generate primary hAT-MSC cultures that gave rise to adherent fibroblast-like cells (Supplementary Fig. 3 Ai) and *in vitro* CFU-Fs (Supplementary Fig. 3 Aii) 2 days and 10 days post-seeding, respectively. AT-derived CFU-F frequency was higher than that reported in BM aspirates (430–600 CFU-Fs/10^6 *versus* 10–100 CFU-Fs/10^6 mononuclear cells seeded), which is still the 'gold standard' for autologous therapy (Castro-Malaspina et al., 1980; Jones and McGonagle, 2008). The hAT-MSC culture at P3 was capable of differentiating towards osteoblasts (Supplementary Fig. 3 Bi & ii), and adipocytes (Supplementary Fig. 3 Biii &iv) in 2-D cultures and towards chondroblasts in 3-D pellet cultures (Supplementary Fig. 3Bv & vi) irrespective of the age of the donor (donor ages 38, 77, 78 years-old). Moreover, the hAT-MSC cultures exhibited a surface marker profile uniformly compatible with the MSC phenotype, with the exception of the CD146 marker, which showed remarkably low levels of expression (Supplementary Fig. 3 C), probably deriving from serial passaging as shown previously for BM-MSCs (Dominici et al., 2006). The hAT-MSC cultures were of high purity being negative for endothelial cell- (CD31) and haematopoietic cell-markers (CD14, CD15, CD45, CD235α) (Supplementary Fig. 4, upper panel) and highly positive (>80%) for major MSC markers (CD29, CD44, CD73, CD105, CD90) [ISCT criteria (Dominici et al., 2006)] (Supplementary Fig. 4, middle panel). Interestingly, hAT-MSCs highly expressed some pericytic markers (CD201, CD140α and CD140β) (Supplementary Fig. 4, bottom panel) directly related to the high vascularity and increased MSC to endothelial cell interactions in adipose tissue (Ryu et al., 2013).

ARTICLE IN PRESS

Moreover, the CD201 expression has been associated with distinct hAT-MSC subsets *in vitro* (Baer et al., 2013). Extensive culturing did not result in chromosomal abnormalities as demonstrated by CGH analysis (Supplementary Fig. 1 A).

Close comparison revealed that hAT-MSCs and hiPSC-MSCs actually exhibit very similar mesenchymal surface marker profiles (Fig. 2C), the only exception being the considerably higher expression of the perivascular marker CD146 (Sacchetti et al., 2007) in hiPSC-MSCs, associating them with vascular smooth muscle commitment and ascribing a myofibroblastic character to the hiPSC-MSCs (Espagnolle et al., 2014). Genome-wide transcriptome comparison of hAT-MSCs and the hiPSC-MSCs revealed that 70% (915 out of 1412) of the up-regulated transcripts during the commitment of hiPSs towards hiPS-MSCs are also found highly expressed in hAT-MSCs compared to pluripotent hiPSCs, supporting the mesenchymal identity of hiPS-MSCs (Supplementary Fig. 5). Indeed, angiogenesis, ossification, connective tissue functions and epithelial to mesenchymal transition (EMT) were among the biological processes that were increased in graphs illustrating the top 200 ($p < 0.005$) biological processes that are enriched in hiPSC-MSCs and hAT-MSCs, when compared to pluripotent hiPSCs (Supplementary Fig. 5 B).

3.3. Generation and validation of the 3-D bioartificial anterior cruciate ligament (baACL)

Though there is a vast choice of biomaterials, we have used the Leeds-Keio biomaterial due to its previous use in orthopaedic operations (Chen et al., 2009). Moreover, both the hAT-MSCs and the hiPS-MSCs showed excellent homing capacity on its fibres 4 days post-seeding, as shown by YOYO-1 staining (Fig. 3A). To generate an implantable bioartificial ACL, we have seeded either hAT-MSCs or hiPSC-MSCs along the entire length (10 cm) of the 3-D biomaterial in Matrigel. In the central 4 cm part, the Matrigel contained TGF-β/FGF-2 for differentiation towards the fibrous ligament, whereas on the last 3 cm of each end of the biomaterial, the Matrigel was supplemented with BMP-2/FGF-2 to develop the osseous bone attachment (Fig. 3B), corresponding to the average dimensions of each part of the normal ACL in humans (Kopf et al., 2011). Confocal and scanning electron microscopy revealed that hAT-MSCs and hiPSC-MSCs, at day 21 post-seeding, had proliferated well on both the fibrous and osseous part the Leeds-Keio biomaterial forming multiple cell layers that started to anastomose into the open pores of the scaffold (Fig. 3C). The high expansion capacity of cells on the biomaterial was also confirmed on the surface of (1 mm and 200 μm images in both left and right panels) and within the individual fibres of the biomaterial (50 μm) (Fig. 3D).

Genome-wide transcriptome analysis of the hAT-MSCs or the hiPSC-MSCs that were induced to differentiate either to the osseous or the ligamentous part of the ACL showed considerable similarity in gene regulation circuits during differentiation. Indeed, differentiation of hAT-MSCs, by TGF-β/FGF-2, towards ligament in the fibrous part of baACL leads to the up- and down-regulation of 183 and 51 genes, respectively (Fig. 3E), whereas differentiation in the osseous part using BMP-2/FGF-2 leads to 191 and 56 genes up- and down-regulated respectively (Fig. 3E). Interestingly, from the up- and down-regulated genes, 179 and 50, respectively, were commonly detected both in the osseous and the fibrous part of the baACL construct. Thus, concerning differentiation of hAT-MSCs to bone there were only 12 and 6 genes that were specifically up- and down-regulated, respectively (Supplementary Table 1), the numbers being even smaller in differentiation of hAT-MSCs to the fibrous part in which only 4 and 1 genes were up- and down-regulated, respectively (Supplementary Table 1). Similarly, a considerable number of genes were commonly regulated in the fibrous and osseous parts of the baACL construct during differentiation of hiPSC-MSCs (Fig. 4E) resulting in a small set of differentially regulated genes (Supplementary Table 2).

3.4. Therapeutic validation of the bioartificial ACL (baACL) in a swine ACL injury model

The baACL generated using hAT-MSCs or hiPSC-MSCs was validated concerning its therapeutic properties using a swine ACL injury model. Towards this purpose, the baACL was transplanted between the attachments of the anteromedial (green in Supplementary Fig. 6) and the posterolateral (purple in Supplementary Fig. 6) bundles of the ACL in order to support the movement of the femoral and tibial bones. After 4 months, PET-CT scanning demonstrated that in all experimental animals, irrespective of whether the baACL was prepared with hAT-MSCs or hiPSC-MSCs, the area of the graft was metabolically active, whereas in the control animal the implantation area was devoid of metabolic turnover (Fig. 4A). Sequencing of PCR-amplified DNA from the baACLs with primers recognising the human TAS1R3 gene, (Fig. 4B) indicated that 4 months after implantation a considerable part of the tissue derives from either the hAT-MSCs or the hiPSC-MSCs. Macroscopically, regenerated ACL had a thickness of 1.5 cm, whereas in control animal (acellular biopolymer only) there was almost no tissue formation and severe osteoarthritic lesions (marked with arrows) in both femoral condyles (Fig. 4C).

Structural evaluation of the reconstructed hAT-MSC or hiPS-MSC ACL showed a triphasic tissue formation (Fig. 4D). Osseous areas consisted of numerous biomaterial fibres embedded within newly formed bone (marked as weak red) and surrounded by mature bone (marked as intense red) (Fig. 4D i). Fibrous areas contained numerous aligned fibres with embedded fibroblasts (Fig. 4D iii) that were surrounded by groups of vessels indicating the blood supply to the newly formed tissue (Fig. 4D iv). Finally, a transition zone was evident in between the fibrous and osseous parts consisting of mature cartilage with embedded chondroblasts (marked with asterisks, Fig. 4D ii). Immunohistochemical evaluation of reconstructed ACL revealed Vimentin and αSMA expression characterising the embedded fibroblasts and the numerous vessels within the fibres, respectively (Fig. 4E). Also, Collagen I and III were present in the fibrous parts of both reconstructed hAT-MSC and hiPS-MSC ACLs being more highly expressed in the latter (Fig. 4E). Importantly, in the implanted baACLs prepared with either hAT-MSCs or hiPSC-MSCs, there was no indication of graft *versus* host disease (GVHD). Indeed, throughout the entire length of the reconstructed ACL in both fibrous and osseous parts, there were no signs of CLA (cutaneous lymphocyte-associated antigen, expressed by T cells of the cutaneous system), CD68 (expressed by monocytes/macrophages) and CD138 (Syndecan-1, expressed by plasma cells) expression (Supplementary Fig. 7). The immunoregulatory and anti-inflammatory properties of MSCs are well documented (Bartholomew et al., 2002; Ghannam et al., 2010).

3.5. Chondrogenic potential of hAT-MSC and hiPS-MSC implants as a validation to reconstruct the transition zone in vivo

Human AT-MSC and hiPS-MSC baACL implant transplantation in a swine ACL injury model resulted in a triphasic tissue formation consisting of fibrous, osseous, and transition zones. Previous studies have shown that physiologically human ACL contains a gradual transition from bone, mineralised fibrocartilage and fibrocartilage, into the ligament substance (Lui et al., 2010). We hypothesised that in our reconstructed ACLs the transition zone originates from the intermediate area between the fibrous and osseous zones of 3-D implant generation model as a result of growth factor influx from both zones. To test this hypothesis in 2-D cultures, hAT-MSCs and hiPS-MSCs were initially induced by all three growth factors involved (TGF-β, BMP-2, FGF-2) in implant generation for 21 days and then differentiated in specialised medium towards chondrogenesis for 15 days (Fig. 5). Both GF induced

Please cite this article as: Kouroupis, D., et al., Generation of stem cell-based bioartificial anterior cruciate ligament (ACL) grafts for effective ACL rupture repair, Stem Cell Res. (2016), http://dx.doi.org/10.1016/j.scr.2016.04.016

hAT-MSC and hiPS-MSC cultures show high sGAG content in 2-D and 3-D micromass chondrogenic conditions at day 15 (Fig. 5A, left and middle panels) and high expression of chondrogenesis-related markers (*SOX9*, *HAPLN1*, *COMP*, *ACAN*, *COL1A2*, *COL3A1*, *COL10A1*) (Fig. 5B; undifferentiated hAT-MSCs and hiPS-MSCs show low expression of chondrogenesis-related markers, data not show). Also, their high

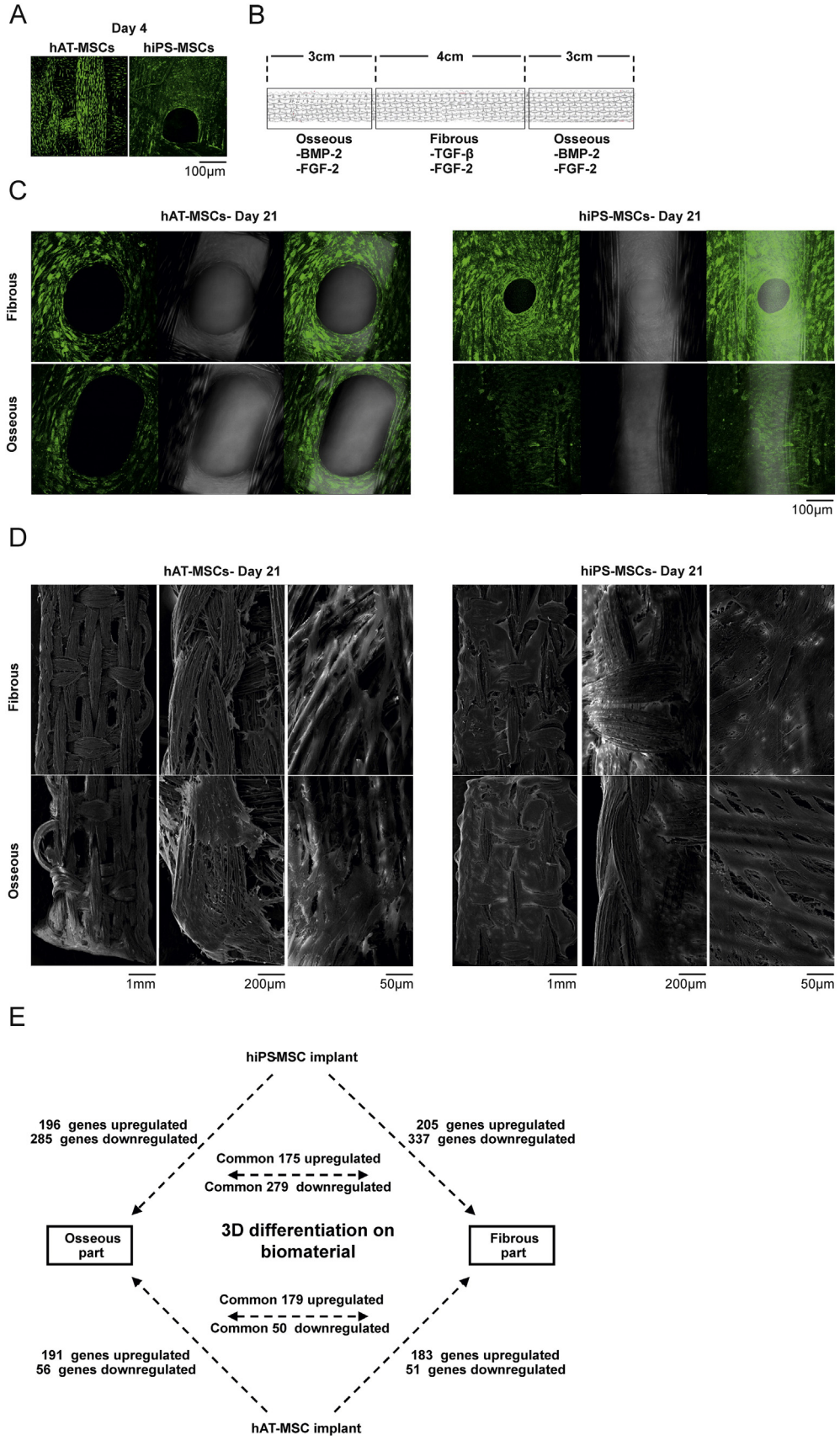

Please cite this article as: Kouroupis, D., et al., Generation of stem cell-based bioartificial anterior cruciate ligament (ACL) grafts for effective ACL rupture repair, Stem Cell Res. (2016), http://dx.doi.org/10.1016/j.scr.2016.04.016

ARTICLE IN PRESS

commitment to chondrogenic fate was evident by very rare ALP$^+$ osteoblasts identified in the culture (right panels). The chondrogenic capacity of the implants generated by 3-D simultaneous differentiation model was also tested. The different zones generated were split and cultured for 15 days in specialised chondrogenic medium (Fig. 5C). Both hAT-MSC and hiPS-MSC implants showed significantly ($p < 0.05$) higher expression of chondrogenesis-related transcripts in osseous or transition zones compared to the fibrous zone. These results reinforce the concept that transition tissue *in vivo* originates from either osseous or transition zones of hAT-MSC and hiPS-MSC implants generated *ex vivo*.

4. Discussion

We have generated bioartificial ACL grafts by differentiating hAT-MSCs or hiPS-MSCs on Leeds-Keio biomaterial to form a ligamentous part in the center and two osseous sections at both ends. We reckoned that ossification on both ends of a baACL would provide stronger attachment on the femur and tibia imitating the origin and insertion of the ACL. Indeed, evaluation using a swine ACL injury model revealed that the generated baACL constitutes a successful proof-of-principle approach for the treatment of ACL rupture that can be used either in repair or reconstruction ACL therapies.

Human AT-MSCs are well-characterised in many studies constituting a solid reference point to compare the efficiency of hiPSC-based cell therapies. The isolated hAT-MSCs complied with the criteria set by the Mesenchymal and Tissue Stem Cell Committee of the International Society for Cellular Therapy (ISCT) (Dominici et al., 2006). We generated hiPSCs from human foreskin fibroblasts (HEFs) using a modification of the footprint-free episomal strategy (Okita et al., 2011). All established hiPS clones were positive for characteristic embryonic markers, their microarray profile was identical to embryonic stem cells (HUES1) and they could generate all three germ layers *in vivo* (Kyrkou et al., in press). Previous published studies have demonstrated the derivation of MSCs from hiPSs through the inhibition of TGF-β pathway (Chen et al., 2012), the supplementation with various growth factors (Niwa et al., 2011) or the induction with MSC-conditioned medium (Lee et al., 2014). In the present study, hiPS-MSCs were derived through alteration of the serum free hiPS medium to a serum-based specialised MSC medium. This simple method resulted in mesengenic progeny possessing the characteristic features of MSCs 20 days post-commitment *in vitro*. These hiPS-MSCs exhibited self-renewal capacity, tripotentiality and MSC-related phenotypic profile.

Direct comparison of hAT-MSC and hiPS-MSC phenotypic profiles exhibited high similarity in expression levels for all mesenchymal, pericytic, haematopoietic and endothelial markers tested. Interestingly, CD324 (E-Cadherin) is highly expressed (~72%) in hiPSC colonies and strongly downregulated (~12%) in hiPSC-MSC post-mesodermal commitment indicating that loss of E-Cadherin-mediated cell–cell contacts occurs during epithelial to mesenchymal transition leading to the acquisition of a mesenchymal phenotype, as expected (Cavallaro and Christofori, 2004; Bates and Mercurio, 2005). In parallel, CD146 (MCAM) expression is strongly increased (from ~46% to 92%) in hiPSC-MSC post-mesodermal commitment suggesting that CD146 is either an inducer of epithelial to mesenchymal transition (Zeng et al., 2012) or simply correlates with an MSC subpopulation located in perivascular tissue niches possessing a vascular smooth muscle phenotype (Espagnolle et al., 2014).

Genome-wide transciptome microarray analysis of hAT-MSCs and hiPS-MSCs revealed high similarity of upregulated transcripts between these mesenchymal populations *versus* the basal pluripotent stem cell state (hiPS). Importantly, a recent study using human platelet serum to establish hiPS-MSCs, revealed a close relationship between MSCs and generated hiPS-MSCs in their global gene expression profile (Frobel et al., 2014). In the present study, the common top 200 ($p < 0.005$) enriched Biological Processes of hAT-MSCs and hiPS-MSCs when compared to the pluripotent background of hiPS indicated an increased tendency of these progenitors to be involved in functional processes related to angiogenesis, ossification, connective tissue formation and epithelial to mesenchymal transition. Similarly, in a previous study hiPSCs commitment to hiPS-MSCs resulted in the upregulation of mesodermal genes (*MSX2*, *NCAM*, *HOXA2*) and downregulation of pluripotency genes (*OCT4*, *LEFTY1/2*) in early cultures (10 days). In the same study, low-throughput microarray analysis of hiPS-MSC late cultures (passage 3) indicated increased expression of genes related to epithelial to mesenchymal transition (Chen et al., 2012). Taken together, these results point to the fact that hiPSC-MSC is a mesenchymal population closely related to hAT-MSCs.

To the best of our knowledge, the simultaneous *in vitro* reconstruction of both fibrous and osseous zones in order to produce a viable baACL construct has not been used before. For this purpose, two growth factor cocktails have been applied, a ligament inducing (TGF-β/FGF-2) in the middle part and a bone forming (BMP-2/FGF-2) in both ends of the biomaterial. Genome-wide transciptome analysis of the ligamentous and osseous zones from hAT-MSC and hiPS-MSC baACLs allowed us to make the following statements. The differentiation of hAT-MSCs to the ligamentous and osseous parts of the biopolymer proceeds with a gene expression pattern that is surprisingly similar. Indeed, when compared to the undifferentiated hAT-MSCs, the up-regulated transcripts in the fibrous (183) and the osseous (191) parts were mostly common (179), even though the inducer was different TGF-β/FGF-2 *vs* BMP-2/FGF-2. The same applied for the down-regulated transcripts too (from the 51 and 56 down-regulated transcripts in the fibrous and osseous parts, respectively, 50 were common). The same was observed in the case of hiPSC-MSCs' transcriptome at the end of fibrous and osseous differentiation on the scaffold *versus* the transcriptome of pre-seeded hiPSC-MSCs, except that the number of the down-regulated transcripts was much higher. Indeed, from the up-/down-regulated transcripts in the fibrous (205/337) and the osseous parts (196/285) the great majority were common (175/279). Considering that both cocktails contain FGF-2 and that BMP-2 activates SMAD1/5/8, an activation that can be also accomplished by TGF-β *via* ALK1, then perhaps such a similarity in the expression pattern is not so surprising. However, the presence of small quantities of BMP-2 are capable of driving the differentiation to bone under these circumstances. In addition, small up-regulation of common ligament- and osteo-related transcripts may be attributed to the specific concentrations used in TGF-β/FGF-2 and BMP-2/FGF-2 cocktails, respectively. In further studies, different growth factor concentrations could yield more striking transcriptome differences between fibrous and osseous parts.

Indeed, both hAT-MSC and hiPS-MSC baACL implants, when validated in a swine ACL excision model, resulted in proper ACL tissue formation. In the osseous zones, both in the tibia and the femur, the fibres of the biomaterial were surrounded by newly formed tissue that was encapsulated within mature bone. Fibrous zones consisted of wavy

Fig. 3. hAT-MSCs and hiPS-MSCs simultaneous 3D differentiation towards osseous and fibrous tissue: A) Both hAT-MSCs or hiPS-MSCs show excellent homing capacity on the Leeds-Keio biomaterial fibres 4 days post-seeding, as shown by YOYO staining of cells' DNA. B) Graphical illustration of the 3-D simultaneous differentiation model on the biomaterial used in our experiments. hAT-MSCs or hiPS-MSCs are initially mixed with Matrigel matrix and differentiation towards fibrous and osseous fates is induced by adding TGF-β/FGF-2 and BMP-2/FGF-2 growth factors in the central and the ends of the biomaterial, respectively. C–D) Confocal microscopy and scanning electron microscopy imaging of hAT-MSCs or hiPS-MSCs on the osseous and fibrous parts of the scaffold. Both hAT-MSCs and hiPS-MSCs show good proliferative capacity by forming multiple cell layers which anastomose into the open-pores of the scaffold. E) Graphical illustration of microarray analysis of hAT-MSCs and hiPS-MSCs post-osteogenic and fibroblastic induction on the biomaterial. In hAT-MSCs, 179 upregulated transcripts and 50 downregulated transcripts were common between the fibrous and osseous parts of the implant. In hiPS-MSC implants, 175 upregulated and 279 downregulated transcripts were common between fibrous and osseous parts of the implant.

Please cite this article as: Kouroupis, D., et al., Generation of stem cell-based bioartificial anterior cruciate ligament (ACL) grafts for effective ACL rupture repair, Stem Cell Res. (2016), http://dx.doi.org/10.1016/j.scr.2016.04.016

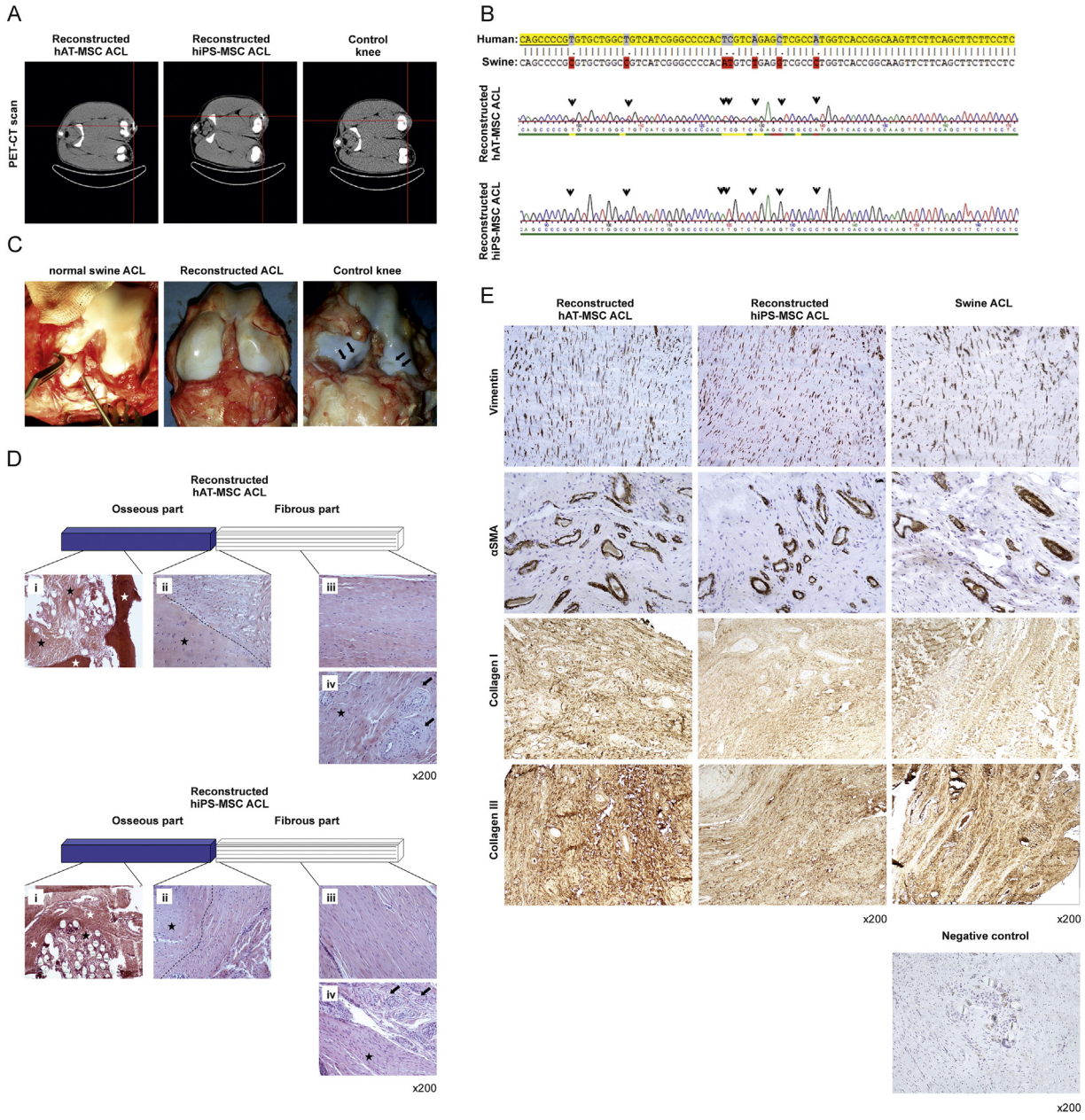

Fig. 4. Anterior cruciate ligament reconstruction with hAT-MSC- or hiPS-MSC-implants 4 months post-implantation in a swine ACL injury model: A) PET-CT scanning showed regeneration only in hAT-MSC and hiPS-MSC implant treated animals (white bands within the area of swine knee joint). B) Nucleotide sequence alignment of TAS1R3 between human and swine species indicates the presence of both species genetic material (dual nucleotide peaks marked with arrows) in reconstructed hAT-MSC and hiPS-MSC ACL tissues. C) Both hAT-MSC and hiPS-MSC implants resulted in *in vivo* reconstruction of ACL tissue. Representative micrographs of normal swine ACL, reconstructed ACL, and control knee. D) Both hAT-MSC and hiPS-MSC implants resulted in the formation of three distinct zones *in vivo*: osseous, fibrous, and transition zones. (i) Osseous zone shows individual bone-forming nodules within both tibia and femur bones consisting of numerous biomaterial fibres surrounded by newly formed osteoblasts (marked with black asterisks) and mature bone (white asterisks). (ii) Transition zone consisting of both cartilaginous area (marked with black asterisk) and Sharpey's fibres area. (iii) Fibrous zone consisting of numerous parallel aligned collagen fibres where individual fibroblasts are embedded. (iv) Multiple vessels are neighbouring the collagen fibres (black arrows). E) Immunophenotyping of hAT-MSC and hiPS-MSC reconstructed ACL tissues reveal positive expression of Vimentin, αSMA, Collagen I and III markers in the fibrous zone of the implants. The negative control is desmin. (For interpretation of the references to colour in this figure, the reader is referred to the web version of this article.)

bundles of Collagen I and III fibres that were infiltrated with numerous Vimentin-positive fibroblasts. Importantly, capillary islets surrounded the collagen fibres, especially in close proximity to the femoral and tibial attachments, indicating a developed blood supply to the newly formed tissue. Thus, both hAT-MSC and hiPS-MSC implants resulted in ACL tissue formation structurally and qualitatively reminiscent of the normal ACL, in comparison to the sole biomaterial implantation which did not result in any significant tissue regeneration. Moreover, 4 months post-baACL graft implantation TAS1R3 gene DNA sequencing of the reconstructed ACL tissue indicated the ample presence of sequences of human origin, whereas the swine genetic material was less but still clearly detectable. Experimental swines uniformly exhibited neither signs of discomfort of the operated knee nor findings of osteoarthritis after sacrifice, in clear distinction to the controls.

Though the results using baACL grafts equipped with hAT-MSCs or hiPSC-MSCs were similar, this does not necessarily indicate the utilisation of common molecular mechanisms. In fact, we have observed striking differences between hAT-MSCs and hiPSC-MSC in the number of genes that were down-regulated during differentiation to the ligamentous (51 *vs* 337) and osseous parts (56 *vs* 285). Also in the up-regulated genes the number of commonly regulated genes was small (16 out of 183/205 in

Please cite this article as: Kouroupis, D., et al., Generation of stem cell-based bioartificial anterior cruciate ligament (ACL) grafts for effective ACL rupture repair, Stem Cell Res. (2016), http://dx.doi.org/10.1016/j.scr.2016.04.016

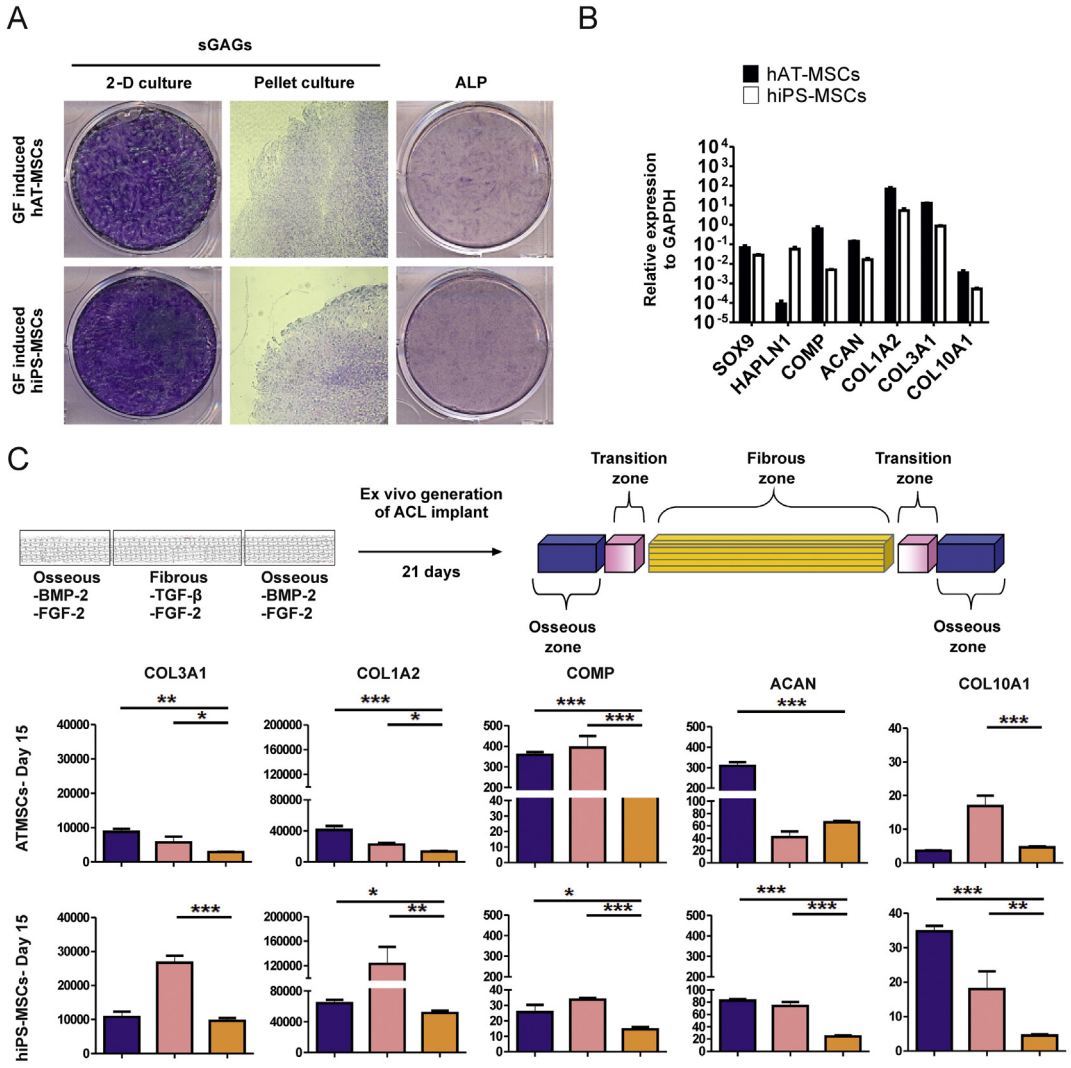

Fig. 5. Generation of cartilaginous transition zone *ex vivo*: A) Chondrogenic differentiation for 15 days of GF-induced (FGF-2/TFGβ/BMP-2) hAT-MSCs and hiPS-MSCs resulted in high sGAGs production in both 2-D (left panel) and micromass (middle panel) cultures. Differentiated cultures show very few alkaline phosphatase (ALP) positive cells (right panel). B) Both GF-induced hAT-MSCs and hiPS-MSCs cultured show upregulated expression of chondrogenic markers (SOX9, HAPLN1, COMP, ACAN, COL1A2, COL3A1, COL10A1) by qPCR. Normalisation of selected transcripts expression levels relative to control GAPDH housekeeping transcript is performed using the formula: $2^{-\Delta Ct}$, ΔCt = Expression value (selected transcript) − expression value (housekeeping transcript). C) Micrograph schematic of three distinct zones generated post-GF induction on the biomaterial *ex vivo*. Subsequent chondrogenic differentiation of separate zones was evaluated using a panel of chondrogenesis-related markers by qPCR. Most markers were significantly (*$p < 0.05$, **$p < 0.01$, ***$p < 0.001$) upregulated in osseous and transition zones.

the ligamentous part and 23 out of 191/196 in the osseous parts). Therefore, it is not impossible to conceive that alternative transcriptional machineries are utilised between hAT-MSCs and hiPSC-MSCs during differentiation to the ligamentous or the osseous parts of the baACL construct. Indeed, hiPSC-MSCs do express high levels of $CD146^{+}$, whereas hAT-MSCs are $CD146^{-}$. CD146 is an endothelial and subendothelial marker (Bardin et al., 1998). Concerning the role of CD146, high expression of CD146 was associated with commitment to a vascular smooth muscle cell (VSMC) lineage, whereas there was no substantial difference in osteogenic, adipogenic and chondrogenic differentiation or *in vitro* haematopoietic supportive activity between $CD146^{-/Low}$ and $CD146^{High}$ MSCs (Espagnolle et al., 2014). However, in a knockdown approach in human MSCs, it was found that CD146 was involved in proliferation and osteogenic differentiation (Stopp et al., 2013). As VSMCs osteogenic differentiate under the influence of the appropriate inducer (Johnson et al., 2006), then differentiation of a $CD146^{+}$ MSC to osteoblast *via* an VSMC intermediate would probably require a different transcriptional programme comparing to a direct differentiation of an $CD146^{-}$ MSC progenitor to osteoblast. Likewise in pathological heterotopic ossification diseases, bone formation outside the skeleton occurs with entirely different mechanisms. This is clearly exemplified by two rare disinherited disorders, the fibrodyslasia ossificans progressiva (FOP) and the progressive osseous heteroplasia (POH). ACVR1 gene mutations are responsible for FOP inducing heterotopic endochondral ossification. POH leads to the generation of predominantly intramembranous bone tissues due to GNAS gene mutations (Shore and Kaplan, 2010).

Tissue-engineered grafts are commonly classified as class III medical devices that require FDA approval for clinical applications. Therefore, many hurdles exist in developing and testing bioartificial grafts for ligament injuries in humans. In our study we successfully tested the baACL grafts in a swine joint that resembles the structure and mechanical forces of the normal human joint. Importantly, both baACL grafts equipped with hAT-MSCs or hiPSC-MSCs showed triphasic tissue structure (fibrous, osseous, transition zones) whereas experimental swines showed no signs of discomfort and osteoarthritis. In further studies, baACL graft generation using animal-free culture conditions and bioabsorbable scaffolds will fullfil FDA requirements. Overall, the present study implies that both hAT-MSC

Please cite this article as: Kouroupis, D., et al., Generation of stem cell-based bioartificial anterior cruciate ligament (ACL) grafts for effective ACL rupture repair, Stem Cell Res. (2016), http://dx.doi.org/10.1016/j.scr.2016.04.016

and hiPS-MSC baACL implants have great potential in future clinical applications.

5. Conclusion

These results provide proof-of-principle data suggesting that stem cells combined with tissue engineering are able to provide solutions that can be applied either to ACL repair or reconstruction therapies. In reconstruction approaches, in which the entire ACL is replaced by a bioartificial ACL the development of approaches to match the anatomical structure of every knee is critical to reduce the postoperative OA. In simple repair, best results concerning the appearance of OA and other long-term consequences will be achievable through the regeneration of the damaged tissue only using stem cells and advanced scaffolds-bridges (scaffolds filling the gaps between the ends of the torn ligaments) (Kiapour and Murray, 2014) without any interference with the local anatomy.

In conclusion, we believe that the present communication clearly indicates that hAT-MSCs and hiPSC-MSCs are both good candidates for the generation of bioarticifial ACL constructs as tested in a swine ACL rupture animal model. Thus, this study supports the idea and provides proof-of-principle evidence that ACL ruptures can be treated using more dynamic and versatile treatment approaches such as those offered by tissue engineering in which the differentiation ability of stem cells is combined with the advanced scaffold technology.

Supplementary data to this article can be found online at http://dx.doi.org/10.1016/j.scr.2016.04.016.

Author contribution

Dimitrios Kouroupis carried out the isolation of hAT-MSCs, the characterisation of hAT-MSCs and hiPSC-MSCs, the tripotentiality protocols, the 3-D differentiation protocol of hAT-MSCs and hiPSC-MSCs. Athena Kyrkou generated hiPSCs and hiPSC-MSCs, and analysed the microarrays of hAT-MSCs and hiPSC-MSCs. Eleni Triantafyllidi and Anna Goussia performed histological analysis of ACL samples. Michalis Katsimpoulas operated the swine ACL rupture models. George Chalepakis performed electron microscopy imaging. Anastasios Georgoulis was the clinical expert of the team and co-initiator of the project together with Theodore Fotsis. Carol Murphy supervised all the experimental work. Theodore Fotsis initiated the project together with Anastasios Georgoulis, he wrote the proposal that supported the funding of the project and he coordinated the work of the entire team as well as the writing of the manuscript.

Acknowledgements

A considerable part of the cost of this study was covered by funds of the National Strategic Reference Framework (NSRF) 2007–2013 (Region of Epirus) (NSRF/2007-13/2011ΕΠ01880025). The title of the funded proposal was “Confronting the Rupture of Anterior Cruciate Ligament: Regeneration using Stem Cells and Tissue Engineering” and T. Fotsis being the principal investigator.

References

Baer, P.C., Kuci, S., Krause, M., et al., 2013. Comprehensive phenotypic characterization of human adipose-derived stromal/stem cells and their subsets by a high throughput technology. Stem Cells Dev. 22 (2), 330–339.

Bardin, N., Frances, V., Combes, V., Sampol, J., Dignat-George, F., 1998. CD146: biosynthesis and production of a soluble form in human cultured endothelial cells. FEBS Lett. 421 (1), 12–14.

Bartholomew, A., Sturgeon, C., Siatskas, M., et al., 2002. Mesenchymal stem cells suppress lymphocyte proliferation in vitro and prolong skin graft survival in vivo. Exp. Hematol. 30 (1), 42.

Bates, R.C., Mercurio, A., 2005. The epithelial-mesenchymal tansition (EMT) and colorectal cancer progression. Cancer Biol. Ther. 4 (4), 371–376.

Castro-Malaspina, H., Gay, R.E., Resnick, G., et al., 1980. Characterization of human bone marrow fibroblast colony-forming cells (CFU-F) and their progeny. Blood 56 (2), 289–301.

Cavallaro, U., Christofori, G., 2004. Cell adhesion and signalling by cadherins and Ig-CAMs in cancer. Nat. Rev. Cancer 4 (2), 118–132.

Chen, J., Xu, J., Wang, A., Zheng, M., 2009. Scaffolds for tendon and ligament repair: review of the efficacy of commercial products. Expert Rev. Med. Devices 6 (1), 61–73.

Chen, Y.S., Pelekanos, R.A., Ellis, R.L., Horne, R., Wolvetang, E.J., Fisk, N.M., 2012. Small molecule mesengenic induction of human induced pluripotent stem cells to generate mesenchymal stem/stromal cells. Stem Cells Transl. Med. 1 (2), 83–95.

Dominici, M., Le Blanc, K., Mueller, I., et al., 2006. Minimal criteria for defining multipotent mesenchymal stromal cells. The International Society for Cellular Therapy position statement. Cytotherapy 8 (4), 315–317.

English, A., Jones, E.A., Henshaw, K., Chapman, T., Emery, P., McGonagle, D.G., 2007. A comparative assessment of cartilage and joint fat pad as a potential source of cells for autologous therapy development in knee osteoarthritis. Rheumatology 46 (11), 1676–1683.

Espagnolle, N., Guilloton, F., Deschaseaux, F., Gadelorge, M., Sensébé, L., Bourin, P., 2014. CD146 expression on mesenchymal stem cells is associated with their vascular smooth muscle commitment. J. Cell. Mol. Med. 18 (1), 104–114.

Frobel, J., Hemeda, H., Lenz, M., et al., 2014. Epigenetic rejuvenation of mesenchymal stromal cells derived from induced pluripotent stem cells. Stem Cell Rep. 3 (3), 414–422.

Ghannam, S., Bouffi, C., Djouad, F., Jorgensen, C., Noel, D., 2010. Immunosuppression by mesenchymal stem cells: mechanisms and clinical applications. Stem Cell Res. Ther. 1 (1), 2.

Johnson, R.C., Leopold, J.A., Loscalzo, J., 2006. Vascular calcification: pathobiological mechanisms and clinical implications. Circ. Res. 99 (10), 1044–1059.

Jones, E., McGonagle, D., 2008. Human bone marrow mesenchymal stem cells in vivo. Rheumatology 47 (2), 126–131.

Jones, E.A., Kinsey, S.E., English, A., et al., 2002. Isolation and characterization of bone marrow multipotential mesenchymal progenitor cells. Arthritis Rheum. 46 (12), 3349–3360.

Kiapour, A.M., Murray, M.M., 2014. Basic science of anterior cruciate ligament injury and repair. Bone Joint Res. 3, 20–31.

Kopf, S., Pombo, M.W., Szczodry, M., Irrgang, J.J., Fu, F.H., 2011. Size variability of the human anterior cruciate ligament insertion sites. Am. J. Sports Med. 39 (1), 108–113.

Kyrkou A, Stellas D, Syrrou M, Klinakis A, Fotsis T, Murphy C. Generation of human induced pluripotent stem cells in defined, feeder-free conditions. Lab. Res. 2016, http://dx.doi.org/10.1016/j.scr.2016.05.006 (in press).

Lee, T.-J., Jang, J., Kang, S., et al., 2014. Mesenchymal stem cell-conditioned medium enhances osteogenic and chondrogenic differentiation of human embryonic stem cells and human induced pluripotent stem cells by mesodermal lineage induction. Tissue Eng. A 20 (7–8), 1306–1313.

Leong, N.L., Petrigliano, F.A., McAllister, D.R., 2013. Current tissue engineering strategies in anterior cruciate ligament reconstruction. J. Biomed. Mater. Res. A 102 (5), 1614–1624.

Li, Z., Qiu, D., Sridharan, I., et al., 2010. Spatially resolved quantification of E-cadherin on target hES cells. J. Phys. Chem. B 114 (8), 2894–2900.

Lui, P., Zhang, P., Chan, K.-M., Qin, L., 2010. Biology and augmentation of tendon-bone insertion repair. J. Orthop. Surg. Res. 5 (1), 59.

Niwa, A., Heike, T., Umeda, K., et al., 2011. A novel serum-free monolayer culture for orderly hematopoietic differentiation of human pluripotent cells via mesodermal progenitors. PLoS ONE 6 (7), e22261.

Okita, K., Matsumura, Y., Sato, Y., et al., 2011. A more efficient method to generate integration-free human iPS cells. Nat. Methods 8 (5), 409–412.

Ryu, Y.-J., Cho, T.-J., Lee, D.-S., Choi, J.-Y., Cho, J., 2013. Phenotypic characterization and in vivo localization of human adipose-derived mesenchymal stem cells. Mol. Cells 35 (6), 557–564.

Sacchetti, B., Funari, A., Michienzi, S., et al., 2007. Self-renewing osteoprogenitors in bone marrow sinusoids can organize a hematopoietic microenvironment. Cell 131 (2), 324–326.

Shore, E.M., Kaplan, F.S., 2010. Inherited human diseases of heterotopic bone formation. Nat. Rev. Rheumatol. 6 (9), 518–527.

Stopp, S., Bornhauser, M., Ugarte, F., et al., 2013. Expression of the melanoma cell adhesion molecule in human mesenchymal stromal cells regulates proliferation, differentiation, and maintenance of hematopoietic stem and progenitor cells. Haematologica 98 (4), 505–513.

Takahashi, K., Yamanaka, S., 2006. Induction of pluripotent stem cells from mouse embryonic and adult fibroblast cultures by defined factors. Cell 126 (4), 663–676.

Zeng, Q., Li, W., Lu, D., et al., 2012. CD146, an epithelial-mesenchymal transition inducer, is associated with triple-negative breast cancer. Proc. Natl. Acad. Sci. 109 (4), 1127–1132.

Zimmerlin, L., Donnenberg, V.S., Rubin, J.P., Donnenberg, A.D., 2013. Mesenchymal markers on human adipose stem/progenitor cells. Cytometry A 83A (1), 134–140.